

Multi-Band CMOS Low Noise Amplifiers Utilizing Transformers

Masataka Kamiyama*, Daiki Oki, Satoru Kawauchi, Seiichi Banba 2)

Nobuo Takahashi, Toru Dan 3), Congbing Li, Haruo Kobayashi

Division of Electronics and Informatics, Gunma University 1-5-1 Tenjin-cho Kiryu 376-8515 Japan

2) Toyohashi University of Technology 3) ON Semiconductor

t14804029@gunma-u.ac.jp k_haruo@el.gunma-u.ac.jp

Abstract— This paper describes multi-band low noise amplifiers (LNAs) utilizing input matching transformers. We investigate a conventional dual-band LNA circuit utilizing a transformer, and show our analysis and simulation results for its circuit. Based on this, we propose a triple band LNA with transformers. We have calculated characteristics of the dual-band and triple-band LNAs. As the results, the LNAs show gain of 20dB maintaining good input matching, in the frequencies at 2.59GHz, 3.50GHz and 5.41 GHz. Then we discuss configuration and design of coupling coefficients of the transformers.

Keywords— CMOS, Low Noise Amplifier, Dual-Band, Triple-Band, Transformer

I. INTRODUCTION

A low noise amplifier (LNA) is used at the front-end of a receiver to amplify a received weak signal with high linearity and noise addition as small as possible

Recently, the wireless receiver is required to be compatible with several wireless standards, such as Bluetooth, WLAN and WiMAX. As each wireless standard has a different frequency band, one receiver is required to handle multi-band signals; there in most cases, multiple LNAs are laid in parallel to realize multi-band receiving ability, however, this method has disadvantages of high power consumption and large chip area. In order to solve these problems, we propose a triple band LNA which integrates multiple bands receiving ability in one LNA, and reduces power consumption and chip area. We have verified the proposed circuit with circuit analysis and Spectre simulations using TSMC 90nm CMOS RF model parameters.

In this paper, we describe multi-band LNAs using transformers. Section II shows Neihart's dual-band LNA [1]. Section III shows our proposed triple-band LNA stimulated by [1], and Section IV shows some consideration of this triple-band LNA layout. Section V concludes this work.

II. NEIHART'S DUAL-BAND LNA WITH A TRANSFORMER

A dual-band LNA using a transformer has been proposed in

[1], and its circuit is illustrated in Fig.1. Cascaded NMOSFETs M1 and M2 are used to enhance the gain, and M3 works as a switch. L_2 and L_G configure a transformer with a coupling coefficient k . We analyze this circuit in the load side and the input matching side separately in the following.

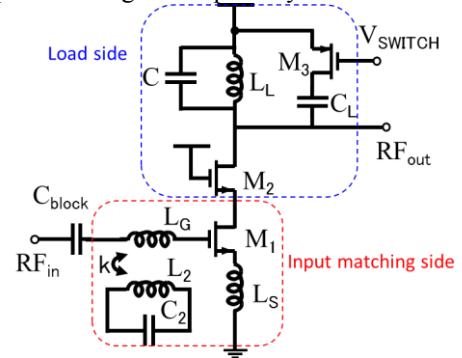


Fig.1. Dual-band LNA circuit utilizing transformer.

A. Load side of the LNA circuit.

The LNA in Fig.1 has two operation modes and VSWITCH determines its operation mode. When VSWITCH is OFF, the resonance frequency is determined by the capacitor C in parallel with the inductor L_L .

$$f_{Load,OFF} : \frac{1}{2\pi\sqrt{L_L \cdot C}} \quad (1)$$

When VSWITCH is ON, the value of the capacitor is changed to $C + C_L$ from C , and the resonance frequency is changed to:

$$f_{Load,ON} : \frac{1}{2\pi\sqrt{L_L \cdot (C + C_L)}} \quad (2)$$

B. Input matching side of the LNA circuit

The small signal equivalent circuit corresponding to the circuit in Fig.1 is shown in Fig.2. Input impedance Z_{in} of the small-signal equivalent circuit is given by the following:

$$Z_{in} = \frac{g_m L_S}{C_{gs}} + j \left\{ \omega(L_g + L_s) - \frac{1}{\omega C_{gs}} + \frac{\omega^3 M^2 C_2}{1 - \omega^2 L_2 C_2} \right\} \quad (3)$$

Here

$$M = k\sqrt{L_g L_2}.$$

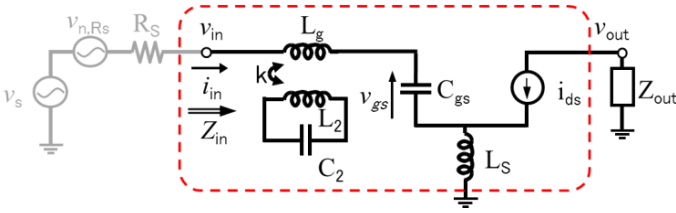


Fig.2. Small-signal equivalent model of dual-band LNA circuit.

In order to satisfy the matching requirement, the real part of equation (3) has to be 50Ω , and the imaginary part has to be 0. In this situation, the resonance frequency has to satisfy the following:

$$\omega(L_g + L_s) - \frac{1}{\omega C_{gs}} + \frac{\omega^3 M^2 C_2}{1 - \omega^2 L_2 C_2} = 0 \quad (4)$$

Then we have the following:

$$\omega^4 (L_g k^2 - L_1) C_{gs} L_2 C_2 + \omega^2 (L_1 C_{gs} + L_2 C_2) - 1 = 0 \quad (5)$$

Where $L_1 = L_g + L_s$

The solutions of this equation are given by

$$\omega = \pm \sqrt{\frac{a^2 + b^2 \mp \sqrt{a^4 + b^4 + a^2 b^2 (4k^2 - 2)}}{2(1 - k^2)}} \quad (6)$$

Where $a = 1/\sqrt{L_1 C_{gs}}$, $b = 1/\sqrt{L_2 C_2}$

Since equation (6) is a quartic equation with even symmetry, its solutions has four real values, two of which are negative and the other two's are positive. We take the two positive values, which are matched to the two resonance frequencies.

〈2·1〉 Spectre simulation

We have performed Spectre simulation of the circuit in Fig.1 with element values in Table 1 and TSMC 90nm CMOS RF model parameters. Simulation results of the input matching characteristics (S11), and the transmission characteristics (S21) are shown in Fig.3.

The dual-band LNA has a low resonance frequency f_{Low} , and a high resonance frequency f_{High} . We see from Fig. 3 that f_{Low} is matched at about 2.5GHz, and f_{High} is matched at about 5.0GHz. The gain at f_{Low} is illustrated in the dotted line, while the gain in f_{High} is shown in the dashed line in Fig.3. We see that the gain of approximately 20dB is obtained by using a respective load. In addition, the gain of close values by switching other loads is obtained, but we observe that it is not possible to take the gain at both of the resonant frequencies at the same time.

Table 1. Dual-band LNA circuit of element values used for

Spectre simulation					
L_G	8.2nH	C_2	700fF	C_{L2}	4pF
L_2	4nH	L_L	1nH	k	0.6
L_S	180pH	C_{L1}	1pF		

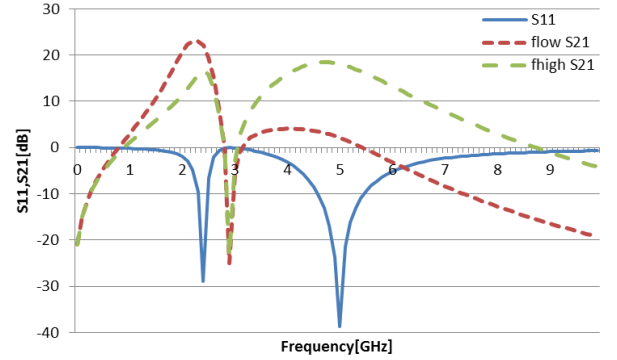
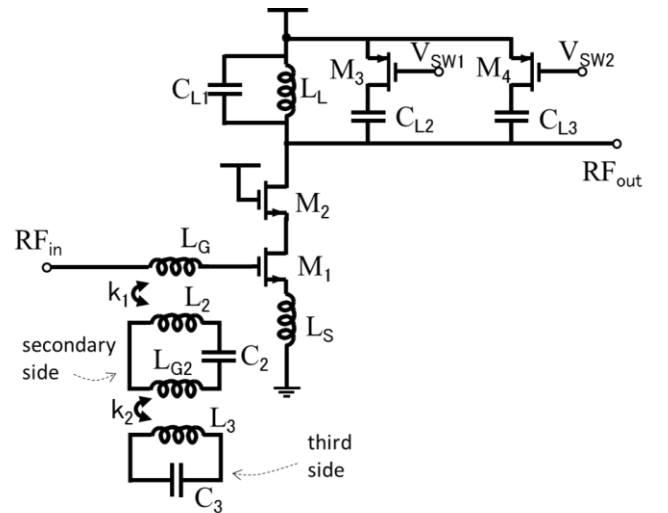


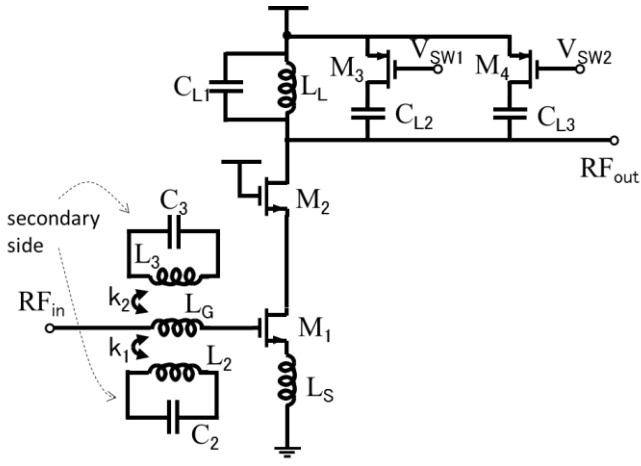
Fig.3. Simulation results of the dual-band LNA.

III. TRIPLE-BAND LNA WITH TRANSFORMERS

We propose here triple-band LNAs using transformers by extending the technique of the dual-band LNA using a transformer described in Section 2. Our proposed LNA circuit uses two transformers; we show two triple-band LNA circuits in Fig.4. Proposed circuit 1 uses transformer couplings between the primary and secondary sides and between the secondary and third sides. Proposed circuit 2 has two transformer couplings with the primary and the secondary sides.



(a) Proposed circuit 1.



(b) Proposed circuit 2.

Fig.4. Proposed triple-band LNA circuits.

By calculating in the same way as in the dual-band LNA circuit case, the input impedance of the proposed circuit 1 is given by

$$Z_{in} = \frac{g_m L_s}{C_{gs}} + j \left\{ \omega(L_g + L_s) - \frac{1}{\omega C_{gs}} \right. \\ \left. + \frac{j\omega^5 M_1^2 C_2 C_3 L_3 - j\omega^3 C_2 M_1^2}{\omega^4 \{C_2 C_3 M_2^2 - C_3 L_3 C_2 (L_2 + L_{g2})\} + \omega^2 \{C_3 L_3 + C_2 (L_2 + L_{g2})\} - 1} \right\} \quad (7)$$

Here

$$M_1 = k_1 \sqrt{L_g L_2}, \quad M_2 = k_2 \sqrt{L_{g2} L_3}.$$

Determining the resonance frequency with zero imaginary part of equation (7) for impedance matching, we have the following:

$$\omega^6 C_{gs} C_2 C_3 \{ (L_g + L_s)(L_2 + L_{g2}) L_3 - (L_g + L_s) k_2^2 L_{g2} L_3 \\ - k_1^2 L_g L_2 L_3 \} \\ + \omega^4 \{ -(L_g + L_s) C_{gs} (L_2 + L_{g2}) C_2 - (L_g + L_s) C_{gs} L_3 C_3 \\ - (L_2 + L_{g2}) C_2 L_3 C_3 + k_2^2 L_{g2} C_2 L_3 C_3 + k_1^2 L_g C_{gs} L_2 C_2 \} \\ + \omega^2 \{ (L_g + L_s) C_{gs} + (L_2 + L_{g2}) C_2 + L_3 C_3 \} - 1 = 0 \quad (8)$$

We obtain a 6-th degree equation for the proposed circuit 2 in a similar manner:

$$\omega^6 \{ (L_g + L_s) C_{gs} L_2 C_2 L_3 C_3 - k_1^2 L_g C_{gs} L_2 C_2 L_3 C_3 \\ - k_2^2 L_{g2} C_{gs} L_2 C_2 L_3 C_3 \} \\ + \omega^4 \{ -(L_g + L_s) C_{gs} L_2 C_2 - L_2 C_2 L_3 C_3 - (L_g + L_s) C_{gs} L_3 C_3 \\ + k_1^2 L_g C_{gs} L_2 C_2 + k_2^2 L_{g2} C_{gs} L_3 C_3 \} \\ + \omega^2 \{ (L_g + L_s) C_{gs} + L_2 C_2 + L_3 C_3 \} - 1 = 0 \quad (9)$$

The formulae for the resonance frequency in the circuits of Fig. 4 are 6-th degree equations (8), (9) with even symmetry.

We see that there are three resonance frequencies of positive values similarly to the dual-band case.

3.1 Spectre simulation

We have performed Spectre simulations for the proposed circuit 1 with element values as shown in Table 2 and TSMC 90nm RF CMOS parameters. Note that LNA load is switched, and we show simulation results in Fig.5 which are mainly properties of the proposed circuit 1, because the proposed circuits 1 and 2 behave similarly.

Hereafter, in triple-band LNAs, we denote f_{Low} as the low resonance frequency, f_{Mid} as the middle resonance frequency and f_{High} as the high resonance frequency. We see in Fig. 5 that impedance matching is obtained at three frequencies, and the gain is obtained at the matched frequencies by utilizing each corresponding load, as the dotted, dashed-long, and dashed lines show.

Table 2. Element values of the proposed triple-band LNA circuit 1 used for Spectre simulation.

Element	Value	Element	Value	Element	Value
L_G	8.2nH	L_S	200pH	C_{L1}	1pF
L_2	4nH	C_2	300fF	C_{L2}	2pF
L_{g2}	4nH	C_3	660fF	C_{L3}	2pF
L_3	4nH	L_L	1nH	k_1, k_2	0.6

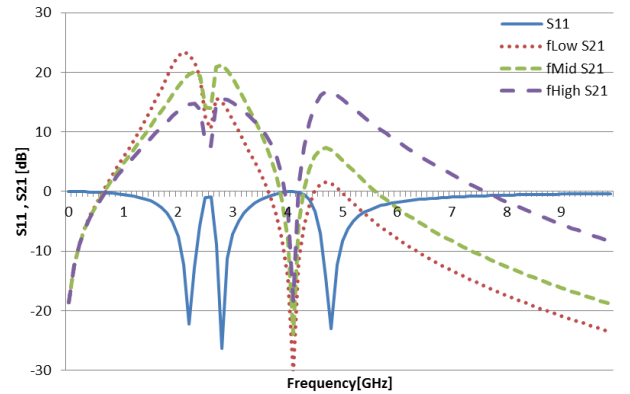


Fig.5. Simulation results of the proposed triple-band LNA circuit 1.

We have calculated the theoretical values for the three resonant frequencies: $f_{Low} = 2.59$ GHz, $f_{Mid} = 3.50$ GHz, $f_{High} = 5.41$ GHz. In order to examine the differences between the ideal and actual MOSFET cases, we have also simulated the input matching characteristics (S11) in the ideal MOSFET case.

The simulation results of S11 in the ideal, the theoretical value and actual element value cases are shown in Fig.6. We see that the resonance frequencies f_{Low} , f_{Mid} , f_{High} match in

the ideal and theoretical value cases respectively, while there are some frequency shifts between the theoretical value and the actual element cases. We consider that the frequency shifts are due to the parasitic capacitor of MOS mainly in the circuit.

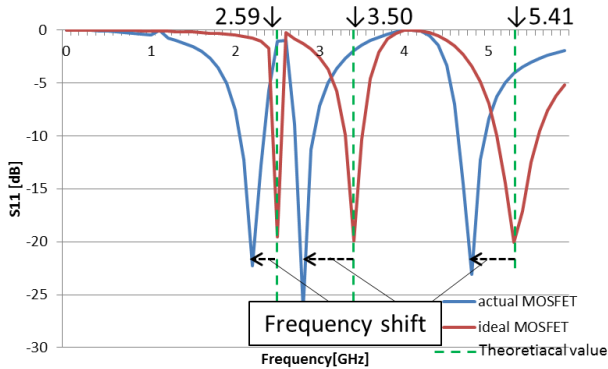


Fig.6. Characteristics comparison for actual elements, theoretical values, and ideal elements cases.

⟨3·2⟩ Coupling coefficient k variation simulation

Proposed circuit 1 in Fig.4 (a) shows how the resonant frequencies change with the coupling coefficient k increase with a step 0.1 at 0-1 area. Two transformers on the triple-band LNA are illustrated here: one is the case that k2 is varying and k1 is fixed, and the other is the case that k1 is varying and k2 is fixed. This simulation was conducted with actual, theoretical element, and theoretical value cases, and its results are shown in Fig.7.

The long-dashed lines (where TSMC 90nm RF CMOS parameters are used) in Fig.7 shows coupling coefficient k1 variation with a fixed k2 and coupling coefficient k2 variation with a fixed k1. The simulation results with ideal elements agree with the theoretical value case. By interchanging k1 and k2, the curve of the actual element shifts a little in frequency axis, which is similar to the curve of the theoretical value.

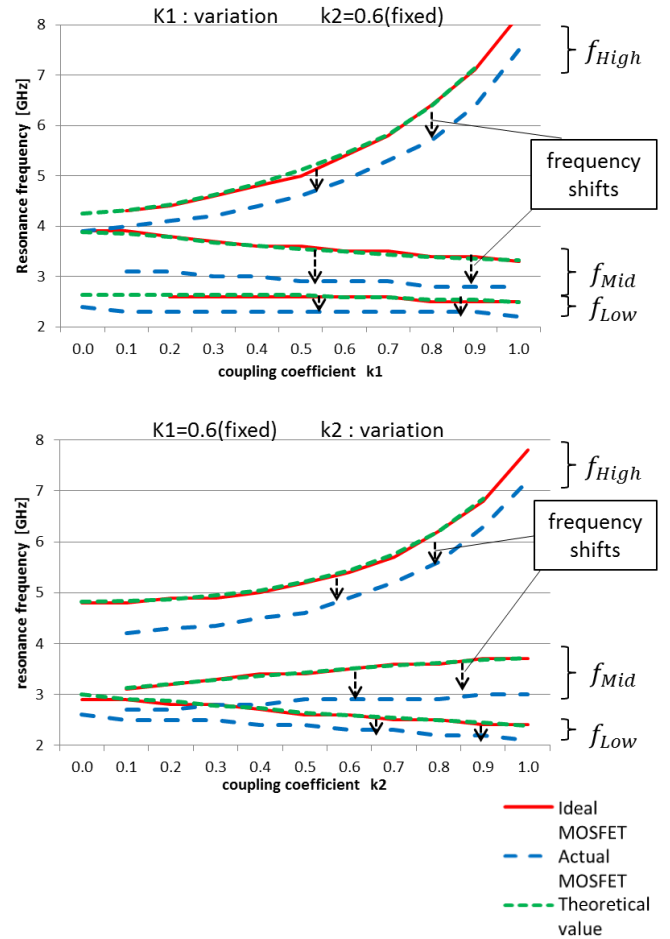


Fig.7. Simulation results for coupling coefficients k1, k2.

⟨3·3⟩ Noise figure simulation

In high frequency circuits, the actual inductor includes parasitic resistance components. Its parasitic resistance value can be calculated from equation (10), and the value of Q is approximately equal to 10. The simulation results of the noise figure are shown in Fig. 9 where parasitic resistance components in all inductors are taken into account.

$$R = \frac{2\pi fL}{Q} \quad (10)$$

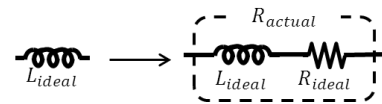


Fig.8. Conversion to actual elements from ideal elements.

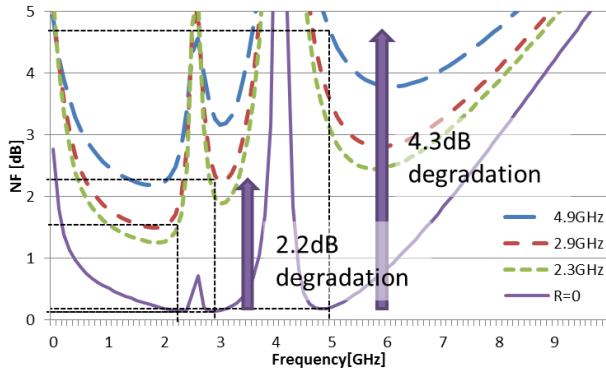


Fig.9. Simulation results for noise figure.

We see that the smaller the NF value is, the fewer the noise components are. We observe in Fig.9 that NF is deteriorated significantly if the resistance components of the inductor are taken into consideration. It is desirable to reduce the deterioration of NF by using CMOS process with inductor $Q > 10$ for high frequency. Also it is necessary to devise the layout, which will be discussed in the next section.

IV. LAYOUT CONSIDERATION OF TRIPLE-BAND LNA

We see that according to NF simulation results, it is necessary to make Q value high in order to prevent degradation of the signal. An inductor or a transformer is usually realized with top layer (which is thick) of the interconnection on a chip for making the inductor Q value high. We propose here two layout methods of the transformer for the triple band LNAs as shown in Fig.10.

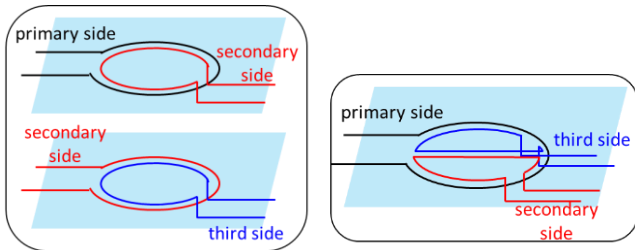


Fig.10. Two layout methods of the transformer.

The left of Fig.10 illustrates the layout method which combines two transformers in sequence. When this method is used, transformers can be created by the top layer on a chip, but it occupies a large chip area. The right of Fig. 10 shows the layout method of combining the second or third side simultaneously to a primary side, and a transformer can be created to the top layer, with a small scale. However there is an issue that it can realize only a small coupling coefficient.

The element values are shown in Table3 when f_{High} reaches

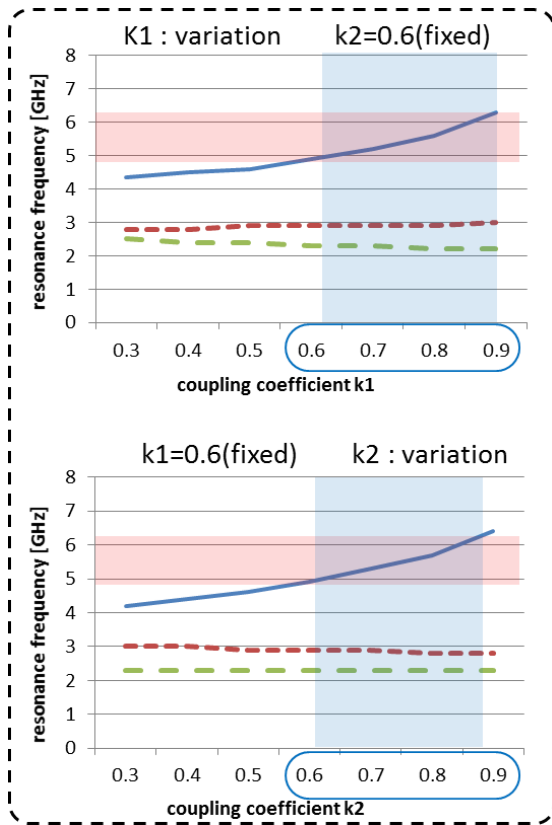
about 5 GHz in the proposed circuits 1, 2. Table 3 shows that, at the resonance frequency of 5 GHz, the proposed circuit 2 can reduce inductor components and coupling coefficient compared with the proposed circuit 1. The coupling coefficients of the proposed circuits 1 and 2 are shown in Fig.11. This graph plots the resonance frequency that is matched. It shows how the coupling coefficient fluctuates when f_{High} reaches about 5~6 GHz. In the proposed circuit 1, another coupling coefficient is fixed $k=0.6$, the varying coupling coefficient is around 0.6~0.9, which is a large value for high resonance frequency. In contrast, in the proposed circuit 2, another coupling coefficient is fixed $k=0.4$, the varying coupling coefficient is around 0.3~0.5, which is a small value for high resonance frequency.

We see from Table 3 and Fig.11 that in order to achieve high resonance frequency with the proposed circuit 1, many inductor components are needed, and the coupling coefficient is high. Therefore, the left-hand side layout of the transformer in Fig.10 is required. On the other hand, the proposed circuit 2 can realize high resonance frequency with fewer inductor components and lower coupling coefficient. So the right-hand side layout of the transformer in Fig.10 can be applied. Thus the proposed circuit 2 can achieve high frequency performance with small chip area.

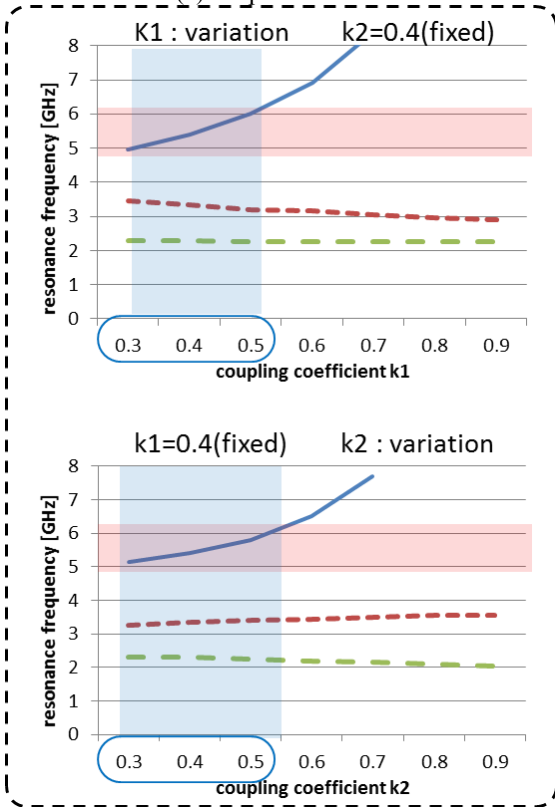
In terms of chip area, it is concluded that proposed circuit 2 is good circuit. On the other hand, in applications that do not mind about the area, proposed circuit 1 also contains a good surface as seen in Fig.11, which shows that f_{High} is slowly responded against variation of coupling coefficient. This advantage leads to ease of design.

Table 3. Element values comparison of proposed circuits 1, 2.

	Proposed 1	Proposed 2
L_G	8.2nH	4nH
L_2	4nH	3nH
L_{g2}	4nH	—
L_3	4nH	5nH
k_1, k_2	0.6	0.4



(a) Proposed circuit 1.



(b) Proposed circuit 2.

Fig.11. Simulation results of coupling coefficient k effects for proposed LNA circuits 1, 2.

V. CONCLUDING REMARKS

We have proposed two structures of triple-band CMOS LNAs using transformers, extending the technique of the dual-band CMOS LNA utilizing a transformer, and we have conducted their circuit analysis and simulation; we see that a triple-band LNA with additional transformer can achieve comparable performance to the corresponding dual-band LNA with a transformer. We have also considered the layout of the transformers for high frequency applications, in order to reduce their chip area.

We are now thinking a multi-band LNA over four. We have confirmed that the number of the resonant frequencies increases by extending this technique. For example, we use three transformers for fourth bands. However, in higher-order cases, it will be difficult to take some resonant frequencies that are aimed. In addition to, other disadvantages exist; these are degradation of NF violently, and appearance of the frequencies that are not matched well. Therefore, the design will be more difficult. We consider from these observations that there is a practical limit to the higher order of expansion in this technology.

Future works are as follows:

- (i) Corresponding electromagnetic field analysis and realization of the transformers.
- (ii) Compensation for the resonance frequency shift.
- (iii) Additional features of higher order multi-band.

Acknowledgements We would like to thank Atsushi Wada for kind support of this research.

- [1] Nathan M. Neihart, Jeremy Brown, Xiaohua Yu : "A Dual-Band 2.45/6 GHz CMOS LNA Utilizing a Dual-Resonant Transformer-Based Matching Network," IEEE, Circuits And Systems I, vol.59, no.8, pp1743-1751, August 2012.
- [2] Kunihiro Asada, Akira Matuzawa : Analog RF CMOS Integrated-Circuit Design Beyond the Basics , Baihuukan, p166-174, (2011-2)
- [3] Hideo Yamamura : Toroidal Core Utilization Encyclopedia, CQ Publisher, p118-126 (2007)
- [4] Shigeo Suzuki : Introduction to High-Frequency Technology, Easy-to-Understand, Nikkann Kougyou Sinnbunnsya, p146-151, (2007)